


Article

Olive Mild Mosaic Virus Coat Protein and P6 Are Suppressors of RNA Silencing, and Their Silencing Confers Resistance against OMMV

Carla MR Varanda ^{1,*} , Patrick Materatski ¹, Maria Doroteia Campos ¹, Maria Ivone E. Clara ², Gustavo Nolasco ³ and Maria do Rosário Félix ²

¹ ICAAM—Instituto de Ciências Agrárias e Ambientais Mediterrânicas, Instituto de Investigação e Formação Avançada, Universidade de Évora, Pólo da Mitra, Ap.94, 7006-554 Évora, Portugal; pmateratski@uevora.pt (P.M.); mdcc@uevora.pt (M.D.C.)

² Departamento de Fitotecnia, ICAAM—Instituto de Ciências Agrárias e Ambientais Mediterrânicas, Escola de Ciências e Tecnologia, Universidade de Évora, Pólo da Mitra, Ap.94, 7006-554 Évora, Portugal; iclara@uevora.pt (M.I.E.C.); mrff@uevora.pt (M.d.R.F.)

³ MeditBio-Centro para os Recursos Biológicos e Alimentos Mediterrânicos, Faculdade de Ciências e Tecnologia, Universidade do Algarve, Campus de Gambelas, 8005-139 Faro, Portugal; gnolasco@ualg.pt

* Correspondence: carlavaranda@uevora.pt

Received: 18 June 2018; Accepted: 6 August 2018; Published: 9 August 2018



Abstract: RNA silencing is an important defense mechanism in plants, yet several plant viruses encode proteins that suppress this mechanism. In this study, the genome of the *Olive mild mosaic virus* (OMMV) was screened for silencing suppressors. The full OMMV cDNA and 5 OMMV open reading frames (ORFs) were cloned into the Gateway binary vector pK7WG2, transformed into *Agrobacterium tumefaciens*, and agroinfiltrated into *N. benthamiana* 16C plants. CP and p6 showed suppressor activity, with CP showing significantly higher activity than p6, yet activity that was lower than the full OMMV, suggesting a complementary action of CP and p6. These viral suppressors were then used to induce OMMV resistance in plants based on RNA silencing. Two hairpin constructs targeting each suppressor were agroinfiltrated in *N. benthamiana* plants, which were then inoculated with OMMV RNA. When silencing of both suppressors was achieved, a significant reduction in viral accumulation and symptom attenuation was observed as compared to those of the controls, as well as to when each construct was used alone, proving them to be effective against OMMV infection. This is the first time that a silencing suppressor was found in a necrovirus, and that two independent proteins act as silencing suppressors in a virus member of the *Tombusviridae* family.

Keywords: RNA silencing; plant protection; resistance; plant viruses; viral suppressors

1. Introduction

RNA silencing is a gene inactivation mechanism identified in most eukaryotes that is involved in several biological processes such as regulating endogenous gene expression, the maintenance of genome stability, and defense against viruses [1,2].

Amongst the several strategies plants have developed to counter virus infections, RNA silencing is one of the most important [1,3]. In antiviral RNA silencing, double-stranded RNAs (dsRNAs) are recognized as foreign and are processed into double-stranded viral short interfering RNAs (siRNAs) that are 21 nt to 22 nt long. Plant virus infections are associated with the accumulation of these virus-specific siRNAs. The cleavage is then accomplished by members of the Argonaute protein family (AGOs) [4] that recruit siRNA and associated proteins to form the RNA-induced silencing complex (RISC). This complex possesses ribonuclease activity and is guided by the single-stranded siRNAs to

its target based on sequence complementarity, resulting in the binding and degradation of homologous RNA molecules [5,6]. Cleavage products of the target RNAs serve as a template of RNA-dependent RNA polymerases (RDR) to form dsRNAs, leading to secondary siRNA production [7], which can again initiate silencing in a self-sustained manner.

To counteract host RNA silencing defense, viruses have evolved several strategies. One such strategy involves viral proteins encoded in the genomes that suppress plant RNA silencing, termed viral suppressors of RNA silencing (VSRs) [8,9]. Most viruses studied have one VSR, and many VSRs have been identified [10]. These proteins are highly divergent, appearing to have evolved independently in the different viruses, and they may interfere in different stages of the RNA silencing pathways, either binding dsRNAs and inhibiting its processing into siRNAs, or sequestering viral siRNAs, preventing their incorporation into RISC or directly interfering with the recognition of viral RNA, dicing, and RISC assembly [6,11].

Viruses from different genera within the *Tombusviridae* family have different suppressors. The p19 protein of tombusviruses *Tomato bushy stunt virus* (TBSV) and *Cymbidium ringspot virus* (CymRSV), which is associated with long-distance movement, is one of the most studied viral suppressors [12–14]. The only function of the p14 protein of the aureusviruses, such as *Pothos latent virus*, seems to be to prevent silencing [15].

The CP of betacarmoviruses such as *Turnip crinkle virus*, as well as the movement proteins of some dianthoviruses, also act as silencing suppressors [16–19]. No silencing suppressors have been identified in the other genera in the family *Tombusviridae*, which would help to elucidate the evolutionary progression of viruses within this family.

The *Olive mild mosaic virus* (OMMV) is a member of the genus *Alphanecrovirus* within the *Tombusviridae* family, and is one of the most spread viruses in olive orchards [20–22]. Its genomic RNA is 3683 nt long with five open reading frames (ORFs), and the virus is likely to have resulted from recombination events between two other necroviruses *Olive latent virus 1* (OLV-1) and *Tobacco necrosis virus D* (TNV-D), based on the high amino acid identity with the RNA-dependent RNA polymerase of OLV-1 and of the CP of TNV-D [23]. ORF1 (p23), pre-readthrough, and ORF2 (p82), predicted as the RdRp, are involved in RNA replication; ORF3 (p8) and ORF4 (p6) are predicted to be involved in virus movement; ORF5 (p29) is predicted as the CP, and it is involved in capsid assembly, systemic movement, and vector transmission [24].

In this study, OMMV-encoded proteins were examined to identify suppressors of RNA silencing and two were found, the CP and p6. OMMV silencing suppression ability seems to result from a coordinate and complementary action of both. In addition, resistance to OMMV in *N. benthamiana* was achieved using hpRNA constructs containing both CP and p6.

2. Materials and Methods

2.1. OMMV Silencing Suppressor Genes

2.1.1. Generation of Constructs

Plasmid DNA containing the viral full-length of an OMMV clone (Accession number HQ651834.1) [25] was used for the amplification of OMMV p23, p82, p8, p6 and CP ORFs as well as full-length OMMV. Each amplified sequence was cloned into pDONRTM221 (Invitrogen, Carlsbad, CA, USA) through a Gateway recombination reaction in accordance with the manufacturer's instructions. The primers used in the reactions are listed in Table 1. Genes were transferred from pDONRTM221 to pK7WG2 binary vector [26] under the promoter CaMV 35S, through LR recombination. Confirmation of the correct sequences was done by sequencing the constructs.

The 2b suppressor gene of *Tomato aspermy virus* (TAV), which was used as positive control, and green fluorescent protein (GFP) (m-gfp5-ER) [27], which was used as a silencing inducer, were cloned as described previously [28].

Binary vectors were transformed into competent *Agrobacterium tumefaciens* strain GV3101/C58C1, carrying pMP90 Ti plasmid, which confers resistance to gentamycin. *A. tumefaciens* cultures were placed individually in 15 mL of Luria-Bertani (LB) medium supplemented with gentamycin, spectinomycin, and rifampicin at 50 µg mL⁻¹ each, 10 mM of MES and 20 µM of acetosyringone. Cultures were then grown at 28 °C and 200 rpm until reaching an OD₆₀₀ of 0.5. Cells were sedimented, re-suspended, in a 3-mL volume containing 10 mM of MgCl₂ (pH 5.6), 10 mM of MES and 100 µM of acetosyringone, and kept in the absence of light at room temperature for 1 h before infiltration [29].

Table 1. Primers used in the Gateway recombination reactions. Recombination sequences specific for the gateway system are underlined. OMMV: *Olive mild mosaic virus*.

Primer Name	Primer (5'-3')	Region Amplified	Location in OMMV Genome	Fragment Length (bp)
attB1	GGGGACAAGTTTGTACAAAAAAGCAGGCT	-	-	-
attB2	GGGGACCACTTTGTACAAGAAAGCTGGGT	-	-	-
OMMVattB1	<u>AAAAAGCAGGCT</u> AGTATACATACCAAGTATA	OMMV	1–19	3707
OMMVattB2	AGAAAGCTGGGTGGGGTCGGGCAAAGGCC		3667–3683	
OMMVp23attB1	<u>AAAAAGCAGGCT</u> AGGATAAAAATGGAGCTCAC	p23	52–70	642
OMMVp23attB2	AGAAAGCTGGGTCTATTGGCCCGAAGGCC		650–669	
OMMVP8attB1	<u>AAAAAGCAGGCT</u> AGGATAAAAATGGAGCTCAC	p82	52–70	2208
OMMVP8attB2	AGAAAGCTGGGTATCAGTTTGTAATCCATTG		2216–2235	
OMMVp8attB1	<u>AAAAAGCAGGCT</u> TTTAATCAATGGATTACCA	p8	2210–2228	267
OMMVp8attB2	AGAAAGCTGGGTACACAGCCATAACTCAAAG		2433–2452	
OMMVp6attB1	<u>AAAAAGCAGGCT</u> CTTTGAGTTATGGCTGTGT	p6	2433–2452	208
OMMVp6attB2	AGAAAGCTGGGTGTCTATTTTGGCATCG		2600–2616	
OMMVCpattB1	<u>AAAAAGCAGGCT</u> ACCAAAACATGCCTAAGAG	CP	2628–2646	842
OMMVCpattB2	AGAAAGCTGGGTTCAAACGTTAATGGTAGGG		3427–3445	

2.1.2. Agrobacterium Co-Infiltration Assays and GFP Imaging

Silencing suppressor assays were based on the previously described system [29]. Briefly, when leaves of *GFP* transgenic 16C line of *N. benthamiana* plants, constitutively expressing the *GFP* gene, are agroinfiltrated with *A. tumefaciens* carrying a *GFP* construct, the green fluorescent signal disappears under UV light due to *GFP* silencing. However, if the *GFP* construct is co-infiltrated with a silencing suppressor, the fluorescence does not disappear, and may even become more intense due to the inhibition of gene silencing caused by the suppressor.

For transient expression assays, *Agrobacterium* cultures carrying each construct were infiltrated into leaves of four-week-old *N. benthamiana* 16C line plants, gently provided by David Baulcombe (University of Cambridge, Cambridge, UK). Single and co-infiltration assays were performed using a 5-mL needleless syringe. Single infiltration consisted of using a 15-mL suspension of *A. tumefaciens* carrying pK_*GFP*. For co-infiltration assays, *Agrobacterium* cultures containing each construct individually, including *Tav-2b*, and *GFP* were mixed in 1:1 *v/v* ratio before agroinfiltration, centrifuged, and resuspended in a final volume of 15 mL.

Three leaves per plant and 10 plants (biological replicates) per each construct were infiltrated. Plants were observed during 12 days post-infiltration (dpi). Each experiment was repeated three times.

The *GFP* fluorescence of infiltrated leaves and whole plants was examined using a long-wavelength UV lamp (UVPBlak-Ray B-100AP, ThermoFisherScientific, Waltham, MA, USA) and photographed with a digital camera (Sony α100 DSLR-A100K, Sony, Tokyo, Japan).

2.1.3. RNA Extraction and Real-Time RT-PCR

Total RNA was extracted from the leaves of three randomly selected agroinfiltrated plants (biological replicates) at 3 dpi, 5 dpi, and 10 dpi, using RNeasy Plant Mini Kit (Qiagen, Hilden, Germany) in accordance with the manufacturer's instructions. The quality and concentration of all of the RNA preparations were determined by using a Nanodrop 2000c spectrophotometer (Thermo Scientific, Waltham, MA, USA).

For reverse transcription, 1 µg of total RNA was used in a 20-µL reaction using Maxima® First Strand cDNA Synthesis Kit for RT-qPCR (Thermo Scientific) in accordance with the manufacturer's instructions.

Primers were designed using Primer Express 3.0 software for real-time PCR (Applied Biosystems, Foster City, CA, USA) using the default parameters for the software (Table 2). Quantitative assays of *GFP* mRNA were performed by real-time RT-PCR (RT-qPCR), carried out on a 7500 Real Time PCR System (Applied Biosystems).

A mRNA *GFP* 147-bp fragment, OMMV ORFs (*p23*, *p82*, *p8*, *p6*, *CP*), as well as full-length OMMV, were amplified. The protein endogenous control genes phosphatase 2A (*PP2*) and F-box protein (*F-box*) were used as internal standards.

RT-qPCRs were carried out with 12.5 µL of 2× SYBR Green PCR Master Mix, 0.3 µM of each primer, and 12.5 ng of cDNA per sample, prepared in 96-well plates and run for 40 amplification cycles comprising a 15-s denaturation at 95 °C, followed by a 1 min at a 60 °C step. A negative control with no template and three technical replicates were considered.

Cycle threshold (C_T) values were determined using the fit-point method and the Applied Biosystems 7500 software with a fluorescence threshold arbitrarily set to 0.1. The relative level of *GFP* mRNA was determined using the amount of *GFP* mRNA from 16C non-inoculated plants as the reference level. At the end of the qPCR, melt curve analysis was conducted to validate the specificity of the primers. A standard curve for each gene was automatically generated by the instrument software (Applied Biosystems) for relative expression level estimation, and data was normalized by *PP2* and *F-box* (reference genes). To exclude the possibility of weak or no silencing suppression due to low levels of the respective protein expression in infiltrated leaves, quantitative assays of the mRNA of each the proteins were performed by RT-qPCR, as described previously for *GFP*.

Table 2. Primers used in RT-qPCR. GFP: green fluorescent protein.

Gene	Primer Name	Primer (5'–3')	Reference
<i>Protein phosphatase 2A</i>	PP2ArtFW	GACCCTGATGTTGATGTTTCGCT	[30]
	PP2ArtREV	GAGGGATTTGAAGAGAGATTTC	
<i>F-box protein</i>	FBOXrtFW	GGCACTCACAAACGTCATTTC	[30]
	FBOXrtREV	ACCTGGGAGGCATCCTGCTTAT	
<i>GFP</i>	GFP-ER Taq-F	GCCAACACTTGTCACTACTTTCTC	[28]
	GFP-ER Taq-R	GTAGTTCCTCGTCCTTGAAG	
<i>OMMV p23</i>	OMMVP23rtFW OMMVP23rtREV	CGAGTCCGCAAGCAGAAGAAG GGGTAGACCAAACCTCGGCA	This study
<i>OMMV p82</i>	OMMVP82rtFW OMMVP82rtREV	TCCAAGACGCCCCGAAAC TGGTTACAGGGGAATGACGC	This study
<i>OMMV p8</i>	OMMVP8rtFW OMMVP8rtREV	GCTCAGAAATCGCAGCAAGG TGTCACGGTAATGGTCTGTCT	This study
<i>OMMV p6</i>	OMMVP6rtFW OMMVP6rtREV	TGTGTCGCTGCTGTGATACTT TTGCAAGGATGAGGATGAGAAT	This study
<i>OMMV CP</i>	OMMVCPrtFW OMMVCPrtREV	TGTCCAGCCACAGCTCTCAT TTCGATGAACTCAATCTCATATCGC	This study

2.1.4. Data Analysis

Univariate and multivariate analyses were performed using the PRIMER v6 software [31] with the permutational analysis of variance (PERMANOVA) add-on package [32], to detect significant differences ($p < 0.05$) in the relative *GFP* mRNA levels between: “ORFs” *p23*, *p82*, *p8*, *p6*, *CP*, OMMV, *GFP* and *Tav-2b*, and “Time” day 3, day 5, and day 10. A two-way PERMANOVA was applied to test the null hypotheses that no significant differences existed between “ORFs” and “Time”.

PERMANOVA analyses were carried out with the following two-factor design: ORFs *p23*, *p82*, *p8*, *p6*, *CP*, OMMV, *GFP*, and *Tav-2b* (eight levels, fixed); and Time, day 3, day 5 and day 10 (three levels, fixed). The data were square root transformed in order to scale down the importance of the high values of relative *GFP* mRNA levels. The PERMANOVA analysis was conducted on a Bray–Curtis similarity matrix [33]. If the number of permutations was lower than 150, the Monte Carlo permutation *p* was used. Whenever significant interaction effects were detected, these were examined using a posteriori pairwise comparisons, using 9999 permutations under a reduced model.

2.2. OMMV Resistance Challenge

A full-length cDNA of OMMV (Accession number HQ651834.1) was used for in vitro transcription using RiboMax™ Large Scale RNA Production System-T7 (Promega, Madison, WI, USA). Following transcription, DNA templates were removed by digestion with DNase, and transcripts were purified by extraction with phenol:chloroform (5:1) acid equilibrated (pH 4.7) (Sigma, St. Louis, MO, USA) and ethanol precipitated.

Synthesized RNA was mechanically inoculated onto six to eight leaf stage *N. benthamiana* plants maintained in a growth chamber at 23 °C with a 16-h photoperiod, for viral propagation. OMMV-infected leaves were then ground in cold 0.1 M of sodium phosphate buffer, pH 6.0 (1:3 *w/v*), which was then filtered, clarified in the presence of organic solvents, concentrated by differential centrifugation, and further purified by ultracentrifugation through sucrose density gradients [34]. The concentration of viral preparations was determined by using a Nanodrop 2000c spectrophotometer (Thermo Scientific) prior to inoculation.

Hairpin constructs of *CP* and *p6* were constructed based on the *CP* without the first 141 nt to exclude *CP*-mediated resistance events (using OMMVCP-141attB1: 5' AAAAAGCAGGCTATC CTAGATCTTCTGGGCTAAGC and OMMVCPattB2) and on the full *p6* (using OMMVp6attB1 and OMMVp6attB2), respectively. hpRNA-*CP* and hpRNA-*p6* constructs were obtained through LR recombination from each pDONR™221-*CP* and pDONR™221-*p6*, as described previously, to pHELLSGATE12 [35], placed in sense and antisense directions to produce self-complementary dsRNAs. Confirmation of the correct sequences was done by sequencing of the constructs after linearization with *Cla*I, which cleaves within the intron.

15 µg of purified OMMV were inoculated onto two fully expanded carborundum-dusted leaves of four-week-old *N. benthamiana* 16C line plants three days after infiltration with *Agrobacterium* cultures carrying pHELLSGATE12-*CP* and pHELLSGATE12-*p6*, as described for transient expression assays. Inoculated plants were grown in the conditions mentioned above. The presence of each construct was confirmed by RT-qPCR at 3dpi, as shown previously.

Ten plants (biological replicates) were infiltrated with pHELLSGATE12-*CP*, 10 were infiltrated with pHELLSGATE12-*p6*, 10 were infiltrated with both constructs, and 10 were infiltrated with the empty vector to be used as negative control. All 40 plants were mechanically inoculated with OMMV. Experiments were repeated two times.

Plants were monitored daily for 30 days for symptom development. A four-grade disease scale was adopted to describe OMMV symptoms along time: 0, no symptoms; 1, mild chlorotic mosaic; 2, intense chlorotic mosaic; 3, necrotic mosaic; 4, pronounced leaf necrosis; and deformation. Disease severity was evaluated at two dpi, five dpi, 10 dpi, and 16 dpi for each batch of plants infiltrated with the different constructs, as follows: Disease Severity Index (DSI) = (SUM of all disease ratings / (Total number of ratings × Maximum disease grade)) × 100.

Total RNAs were extracted from upper non-inoculated leaves from three randomly selected plants (biological replicates), at five dpi and 16 dpi. Virus accumulation was determined by quantitative real time PCR analysis using OMMVp23 primers (Table 2), as described above.

Univariate and multivariate analyses were performed as described above, using the PRIMER software to detect significant differences ($p < 0.05$) in the virus accumulation between; “ORFs” *p6*, *CP*, and *p6 + CP*, and “Time” five dpi and 16 dpi. A two-way PERMANOVA was applied to test the

null hypotheses that no significant differences existed between “ORFs” and “Time”. PERMANOVA analyses were carried out as previously, with the following two-factor design: ORFs *p6*, *CP*, and *p6 + CP* (three levels, fixed); and Time five dpi and 16 dpi (two levels, fixed). The data were square-root transformed in order to scale down the importance of the high values of virus accumulation.

3. Results

3.1. Determination of OMMV Silencing Suppressors

To identify potential OMMV RNA silencing suppressors, all of the proteins encoded by the genome were tested for their ability to suppress silencing by using a *GFP* reporter gene in plant tissues. Individual OMMV ORFs were cloned into a binary vector (pK7WG2) driven by the CaMV 35S promoter in *A. tumefaciens*. For comparison, a full-length cDNA clone of OMMV that generates a full infection in *N. benthamiana* was also cloned. Transient expression assays were performed on transgenic 16C *N. benthamiana* plants by co-infiltrations of each clone plus pK_ *GFP*, a construct that expresses a transcript homologous to the transgene of 16C plants.

Infiltrated *N. benthamiana* leaf patches showed GFP fluorescence under UV light at two dpi in all of the samples (data not shown). Leaves infiltrated with the silencing inducer pK_ *GFP* showed a weak GFP fluorescence at three dpi (Figure 1, GFP 3dpi) and at five dpi, fluorescence disappeared (Figure 1, GFP 5 dpi) and silencing began, as seen by the development of a red color under UV light on the infiltrated region.

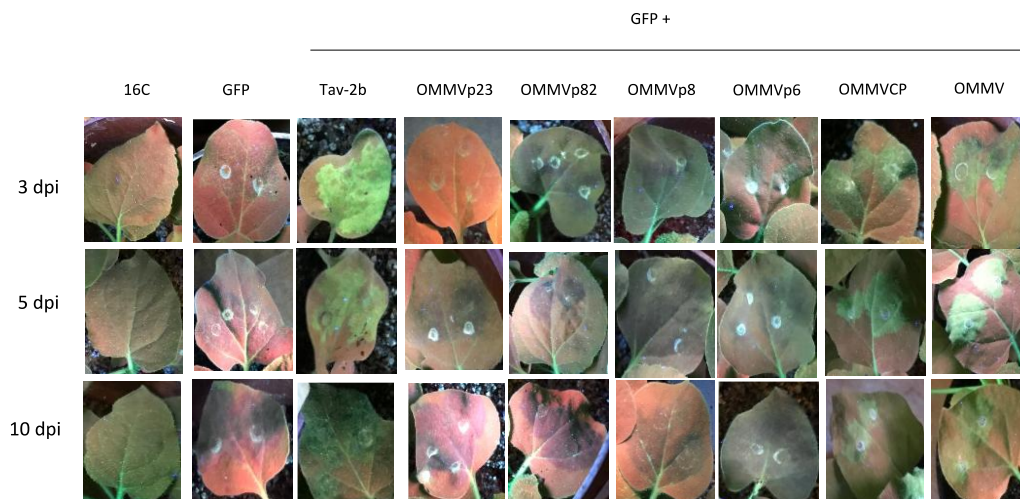


Figure 1. Visual observation of leaves from transgenic *N. benthamiana* 16C plants under UV light at three, five, and 10 days post-infiltration (dpi). Non-infiltrated (16C), infiltrated with *Agrobacterium tumefaciens* harboring pK-*GFP* alone (GFP), and co-infiltrated with pK-*GFP* plus: *Tav-2b*, OMMVp23, OMMVp82, OMMVp8, OMMVp6, OMMVCP, and OMMV.

In the positive control, leaves co-infiltrated with pK_ *GFP* and the strong suppressor *Tav-2b* presented bright fluorescence at three dpi (Figure 1, *Tav-2b* 3 dpi), and fluorescence was maintained for the next seven days, although it was less intense (Figure 1, *Tav-2b* 10 dpi).

In the co-expression of OMMVp23, OMMVp82, and OMMVp8, at three dpi, five dpi, and 10 dpi, no fluorescence was observed under UV light, and silencing began at five dpi and was maintained at 10 dpi.

At three dpi, five dpi, and 10 dpi, OMMVp6, OMMVCP, and OMMV were able to suppress *GFP* silencing, as seen by the green fluorescence under UV light.

OMMVCP and OMMV showed the most intense suppressor activity at five dpi, whereas OMMVp6 showed the most intense suppressor activity at three dpi. However, OMMVp6 green fluorescence

showed lower intensity at all times when compared to OMMVCP and OMMV, and was almost undetectable at 10 dpi.

GFP fluorescence in the presence of pk_OMMV was reproducibly stronger than with each of the viral genes, and was similar to the levels observed for Tav-2b. However, in contrast to Tav-2b, where higher levels were observed at three dpi, a brighter fluorescence was observed at five dpi.

Monitoring of upper non-infiltrated leaves showed systemic silencing at 15 dpi in all of the samples, suggesting that OMMVp6 and OMMVCP possess suppressor local RNA silencing activity, but cannot suppress systemic silencing.

RT-qPCR showed that all of the samples presented C_T values within the linear calibration curves. Two reference genes (*PP2* and *F-box*) were used to normalize the expression of target genes. The amplification efficiency and correlation coefficient (R^2) of their calibration curves were 107.25% and 0.9943% for *PP2*, and 99.62% and 0.9978% for *F-box*.

PERMANOVA analysis revealed significant differences in the factors “ORFs” and “Time” ($p < 0.0001$). In addition, a significant interaction occurred between the two factors (“ORFs” and “Time”) ($p < 0.0001$). As expected by visual observations, RT-qPCR at three dpi showed the highest values (mean \pm SE) of relative GFP mRNA levels; 2.50 ± 0.01 in Tav-2b gene, followed by 2.41 ± 0.01 in OMMV, 2.10 ± 0.005 in CP, and 1.60 ± 0.004 in p6 (Figure 2). Individual pairwise comparisons at three dpi revealed a high variability of relative GFP mRNA levels with significant differences between most ORFs ($p < 0.05$) (Table 3). Individual pairwise comparisons showed no significant differences between: *p* GFP versus *p*23 > 0.9153 , *p* p23 versus *p*82 > 0.6178 and *p* p23 versus *p*82 > 0.088 .

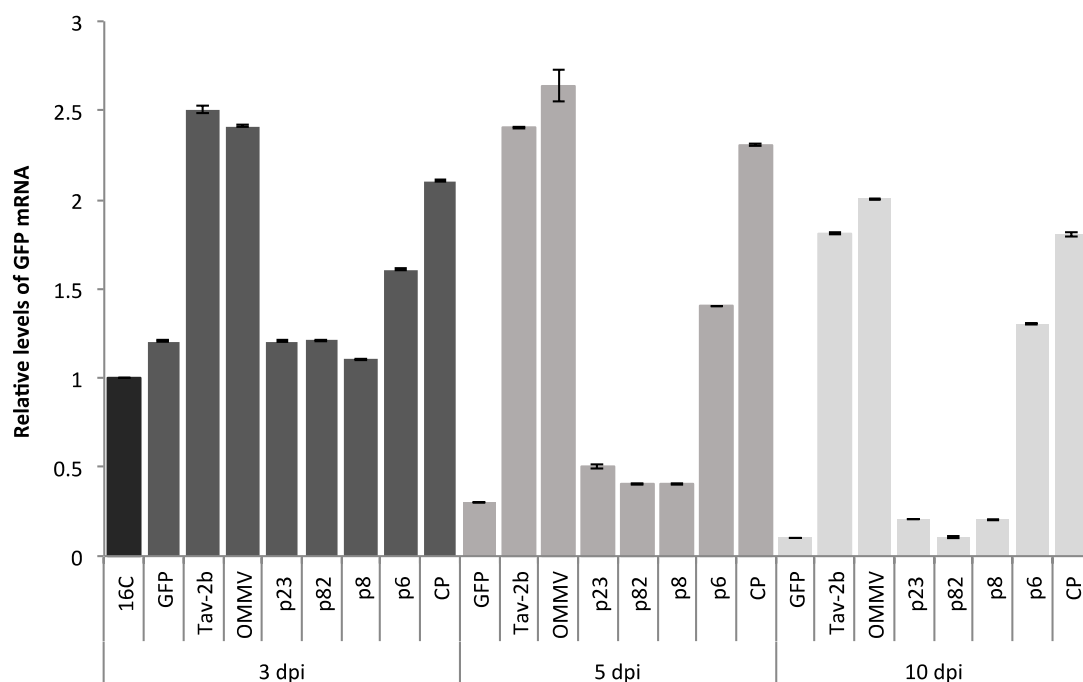


Figure 2. Mean relative levels of GFP mRNA \pm standard error (SE) obtained from three infiltrated 16C *N. benthamiana* plants (biological replicates) at three dpi, five dpi, and 10 dpi, determined by RT-qPCR and normalized by the levels of phosphatase 2A (*PP2*) and F-box protein (*F-box*) reference genes. 16C: 16C non-inoculated plants; GFP: single infiltration with pk_GFP; Tav-2b, OMMVp23, OMMVp82, OMMVp8, OMMVp6, OMMVCP, and OMMV: co-infiltration of pk_GFP with the corresponding constructs. The GFP transgene level in non-infiltrated *N. benthamiana* 16C plants was used as a standard and given a value of 1.

At five dpi, RT-qPCR showed a great reduction in GFP mRNA levels in the presence of GFP alone or in the presence of OMMVp23, OMMVp82, and OMMVp8. Consistent with visual observations,

at five dpi, the highest values (mean \pm SE) of relative *GFP* mRNA levels were 2.64 ± 0.09 in OMMV (1.6-fold greater than non-infiltrated 16C at five dpi), followed by 2.40 ± 0.005 in *Tav-2b*, 2.30 ± 0.004 in *CP*, and 1.40 ± 0.002 in *p6* (Figure 2). Individual pairwise comparisons at five dpi revealed a high variability of relative *GFP* mRNA levels with significant differences between most of the ORFs ($p < 0.05$) (Table 3). Individual pairwise comparisons revealed no significant differences between: *p Tav-2b* versus OMMV > 0.0518 and *p p82* versus *p8* > 0.9977 .

At 10 dpi, all of the *GFP* levels decreased, the highest values (mean \pm SE) of relative *GFP* mRNA levels were 2.00 ± 0.005 in OMMV, followed by 1.81 ± 0.005 in *Tav-2b*, 1.80 ± 0.01 in *CP*, and 1.30 ± 0.003 in *p6* (Figure 2) (from 0.3 in OMMV *p6* to onefold greater than non-infiltrated 16C plants in OMMV). Individual pairwise comparisons at 10 dpi revealed a high variability of relative *GFP* mRNA levels with significant differences between most of the ORFs ($p < 0.05$) (Table 3). Individual pairwise comparisons revealed no significant differences between: *p GFP* versus *p82* > 0.3574 , *p p23* versus *p82* > 0.6807 , *p p23* versus *p8* > 0.6569 , *p p82* versus *p8* > 0.6799 and *p Tav-2b* versus *CP* > 0.8368 .

Plants co-infiltrated with *pk_GFP* and OMMV *CP* and *pK_GFP* and OMMV maintained the greenish patch for 11 and 14 days, respectively.

At three dpi and five dpi, expression in leaves co-infiltrated with *pk_GFP* and each OMMV *p23*, OMMV *p82*, OMMV *p8*, and OMMV *p6*, was similar to that of the strong silencing suppressor OMMV *CP*. This result confirms that proteins were being expressed, and demonstrated that weak or no silencing suppression was not due to low protein expression.

Table 3. Details of the two-factor permutational analysis of variance (PERMANOVA) pairwise tests with open reading frames (“ORFs”) (eight levels, fixed) and “Time” (three levels, fixed) for all of the analyzed variables. Bold values highlight significant effects ($p < 0.05$).

Pairwise Tests	3 dpi	5 dpi	10 dpi
ORFs			
<i>GFP</i> vs. <i>Tav-2b</i>	0.0001	0.0001	0.0001
<i>GFP</i> vs. OMMV	0.0001	0.0001	0.0001
<i>GFP</i> vs. <i>p23</i>	0.9153	0.0001	0.0001
<i>GFP</i> vs. <i>p82</i>	0.6178	0.0001	0.3574
<i>GFP</i> vs. <i>p8</i>	0.0002	0.0001	0.0001
<i>GFP</i> vs. <i>p6</i>	0.0001	0.0001	0.0001
<i>GFP</i> vs. <i>CP</i>	0.0001	0.0001	0.0001
<i>Tav-2b</i> vs. OMMV	0.0129	0.0518	0.0001
<i>Tav-2b</i> vs. <i>p23</i>	0.0001	0.0001	0.0001
<i>Tav-2b</i> vs. <i>p82</i>	0.0001	0.0001	0.0001
<i>Tav-2b</i> vs. <i>p8</i>	0.0001	0.0001	0.0001
<i>Tav-2b</i> vs. <i>p6</i>	0.0001	0.0001	0.0001
<i>Tav-2b</i> vs. <i>CP</i>	0.0001	0.0004	0.8368
OMMV vs. <i>p23</i>	0.0001	0.0001	0.0001
OMMV vs. <i>p82</i>	0.0001	0.0001	0.0001
OMMV vs. <i>p8</i>	0.0001	0.0001	0.0001
OMMV vs. <i>p6</i>	0.0001	0.0002	0.0001
OMMV vs. <i>CP</i>	0.0001	0.0134	0.0001
<i>p23</i> vs. <i>p82</i>	0.6137	0.0016	0.6807
<i>p23</i> vs. <i>p8</i>	0.0001	0.0017	0.6569
<i>p23</i> vs. <i>p6</i>	0.0001	0.0001	0.0001
<i>p23</i> vs. <i>CP</i>	0.0001	0.0001	0.0001
<i>p82</i> vs. <i>p8</i>	0.0001	0.9977	0.6799
<i>p82</i> vs. <i>p6</i>	0.0001	0.0001	0.0001
<i>GFP</i> vs. <i>Tav-2b</i>	0.0001	0.0001	0.0001
<i>GFP</i> vs. OMMV	0.0001	0.0001	0.0001
<i>GFP</i> vs. <i>p23</i>	0.0001	0.0001	0.0001
<i>GFP</i> vs. <i>p82</i>	0.0001	0.0001	0.0001

3.2. OMMV Resistance Challenge

The presence of each construct was confirmed by RT-qPCR at three dpi in plants infiltrated with *Agrobacterium* cultures carrying the constructs.

The appearance of disease symptoms was monitored at two dpi, five dpi, 10 dpi, and 16 dpi and recorded as a disease index scale. As shown in Figure 3, at two dpi, plants expressing OMMV CP, OMMV *p6*, and both OMMV CP and *p6* did not show any symptoms, whereas two plants in negative control showed mild symptoms (DSI, 5%). At five dpi, plants from all groups showed symptoms, but only a few plants in the negative control group reached the disease index scale of 2, presenting the highest DSI (32.5%), followed by plants expressing *p6* alone (22.5%). At 10 dpi and 16 dpi, control plants showed severe symptoms (DSI 75% and 100%, respectively). Plants expressing OMMV *p6* showed a slight lower DSI at 10 dpi (60%), but also reached 100% at 16 dpi, showing only a delay in the appearance of symptoms. At the same time points, plants expressing OMMV CP presented considerably lower DSIs (32.5% and 57.5%), indicating a tolerance to OMMV infection. In contrast, plants expressing both OMMV CP and *p6* showed a maximum DSI of 20% at 16 dpi, indicating a very high tolerance to OMMV infection. Additionally, in the experiments, an average of 60% of the plants expressing OMMV CP and *p6* did not present any viral symptoms at 16 dpi, suggesting a resistance to OMMV. Plants expressing OMMV CP also showed some resistance, although in a lower level (20%). Plants were monitored until 30 dpi, and the highest DSI was 60% in plants expressing OMMV CP, and 30% in plants expressing both OMMV CP and *p6*, no plants reaching the maximum disease index.

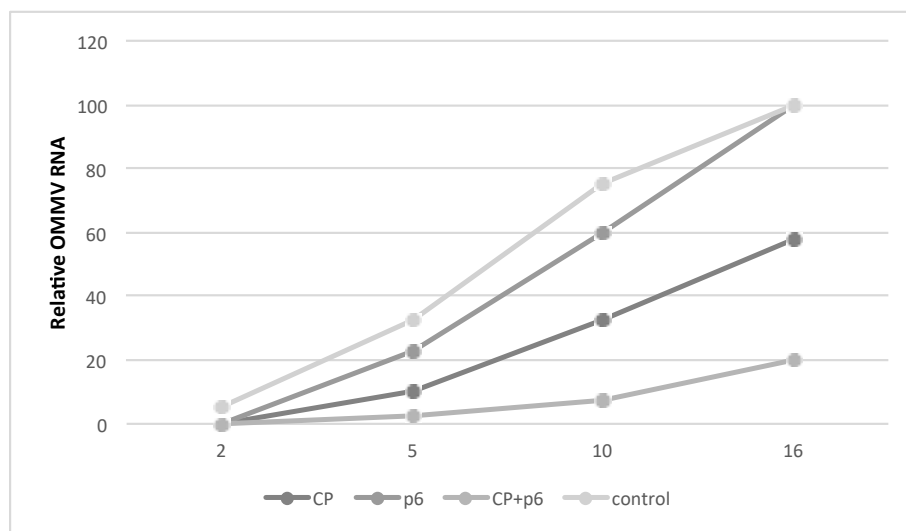


Figure 3. Disease severity of plants (10 biological replicates) expressing OMMV CP, OMMV *p6*, OMMVCP + *p6*, and negative control at two dpi, five dpi, 10 dpi, and 16 days after inoculation of OMMV.

Viral accumulation levels were determined by real time RT-qPCR (Figure 4), and the results are consistent with the disease severity symptoms observed. At five dpi, the mean viral accumulation \pm SE in the upper non-inoculated leaves of plants expressing OMMVCP + *p6* was 0.0 , 11.0 ± 2 in OMMVCP, 28.5 ± 0.5 in OMMV*p6*, and 52.5 ± 2.5 in plants expressing the empty vector. Individual pairwise comparisons revealed significant differences ($p < 0.01$) between all of the treatments. At 16 dpi, the mean viral accumulation \pm SE in the upper non-inoculated leaves of plants expressing OMMVCP + *p6* was 17.5 ± 2.5 , 119.0 ± 1.0 in OMMVCP, 197.5 ± 2.5 in OMMV*p6*, and 200.0 ± 0.0 in plants expressing the empty vector. Individual pairwise comparisons revealed significant differences between empty vector versus OMMVCP ($p < 0.008$); empty vector versus OMMVCP + *p6* ($p < 0.0032$); OMMVCP versus OMMV*p6* ($p < 0.0011$); OMMVCP versus OMMVCP + *p6* ($p < 0.005$), and OMMVCP + *p6* versus

OMMV ($p < 0.0029$). No significant differences were found between empty vector and OMMV ($p > 0.4205$).

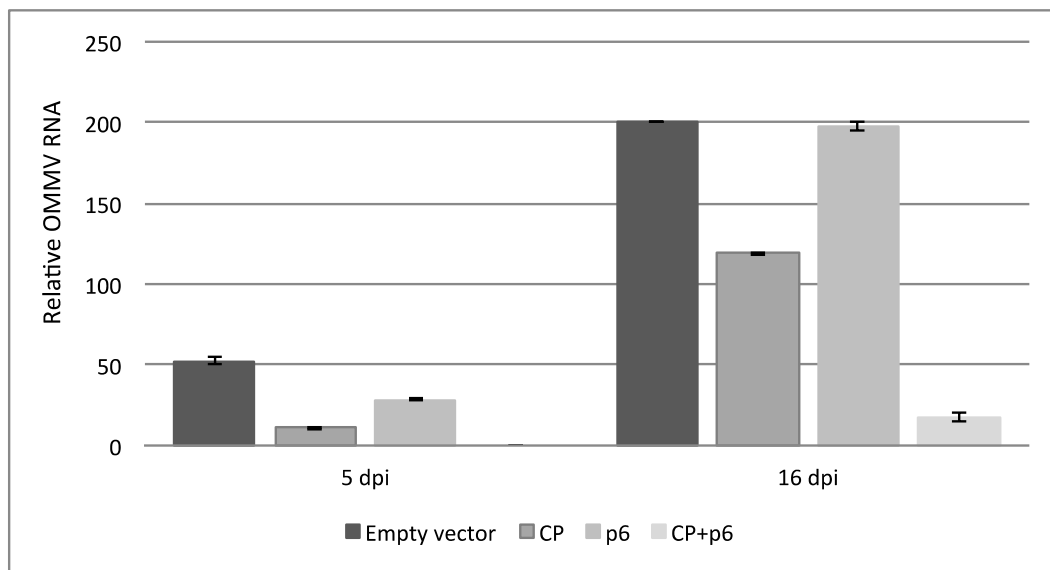


Figure 4. Viral accumulation levels in upper non-inoculated leaves of three biological replicates, at five and 16 days after OMMV inoculation.

Both visual observations and quantitative RT-PCR indicate that OMMV *CP*, and remarkably OMMV *CP* together with *p6*, attenuate viral symptoms and reduce viral accumulation levels.

4. Discussion

Most plant viruses have evolved by encoding one or more silencing suppressors as a counter-response to the antiviral plant gene silencing defense mechanism [9]. Members of the *Tombusviridae* family share common features, but show different strategies to suppress silencing. Tombusviruses p19 protein, the equivalent p14 protein of the aureusviruses, the replicase proteins of the dianthoviruses, and the CP of the carmoviruses (alpha and beta) have been identified as *Tombusviridae* silencing suppressors.

Members of the *Tombusviridae* family present a high diversity of viral suppressors. The closest related genera, the carmoviruses, use the *CP* as silencing suppressor. However, in opposition to the carmoviruses *CP*, the *CP* of necroviruses lacks a protruding domain, and has low similarity to the *CP* of carmoviruses. In addition, the genome of OMMV does not present proteins equivalent to tombusviruses p19 and aureusviruses p14, and the necroviruses replicase has a very low similarity to the replicase of the dianthoviruses [36].

In this study, the complete OMMV genome was screened for the presence of a gene with potential RNA silencing suppression activity. Co-infiltration assays using the *N. benthamiana* 16C line, *GFP*-transformed, revealed that the full genome of OMMV encodes RNA silencing suppressors with activity similar to the strong suppressor *Tav-2b*. When each of the individual proteins were tested separately, *CP* and *p6* were capable of inhibiting *dsGFP*-induced local silencing, at different levels. However, this was lower than when the entire genome was used, as seen by enhanced *GFP* fluorescence and *GFP* mRNA levels. Despite no experiments having been done using a combination of *p6* and *CP*, the other ORFs not showing a suppressor activity seems to suggest that OMMV silencing suppression-enhanced activity is due to a coordinate and complementary action of both *CP* and *p6* as silencing suppressors. The analysis of each protein separately demonstrated that most suppressor activity is due to the *CP*, with *p6* showing a much lower inhibition of local RNA silencing.

This finding is in line with previous data on OMMV mutants containing several changes in *CP* sequence, which exhibited different levels of symptoms in indicator plants, suggesting a clear role of that protein in symptom modulation [24].

The combination of several functions in the same protein may be advantageous for the virus.

This is the first time that two independent proteins were found to act as silencing suppressors in a member of the *Tombusviridae* family similarly to that shown in some members of *Closteroviridae* [37] and *Filoviridae* [38].

The existence of different viral suppressor proteins in one virus seems to be an advantage in targeting different pathways of host defense at the cellular level as it allows for a more successful host infection. Viruses with single suppressors may only gain this advantage in mixed infections with others that possess distinct silencing suppressors with different targeting modes, thus causing a more effective interference with the plant defense mechanism that results in increased symptoms, higher viral accumulation, and favoring cell-to-cell movement [39–41]. This has been observed with PVX and CMV that encode distinct suppressors that target both intracellular and intercellular silencing, leading to enhanced viral accumulation and symptoms characteristic of synergistic effect, in double infections [42].

Synergistic effects have been seen between OMMV and the close related OLV-1 during co-infection. OMMV is only acquired from the soil when OLV-1 is present, in which case both viruses are able to invade the plant and spread throughout the plant, causing systemic symptoms instead of the typical local lesions induced by each virus separately [43]. In fact, it is interesting to notice that both OMMV silencing suppressors are predicted to be involved in movement: *p6* in cell-to-cell movement, and *CP* in systemic movement [44].

The discovery of OMMV viral suppressors have prompted us to explore their use in the development of OMMV-resistant plants through pathogen-derived resistance (PDR) based on RNA silencing.

The development of viral resistant plants has been a matter of study for many years and different levels of resistance have been obtained varying with the type of molecules and viral genome region used to trigger RNA silencing [45–47]. As an alternative to transgenic plants and to overcome their associated biosafety and legislative constraints, transient RNA silencing systems have been developed consisting on the direct delivering of different RNA silencing molecules into plants [48–50].

The expression of self-complementary hairpin-RNA, in opposition to single-sense or antisense constructs, induces a high level of RNA silencing in plants due to the production of dsRNA through the transcription of the hairpin structure; in addition, the presence of an intron in between the complementary regions stabilizes the construct and enhances silencing efficiency [51–53].

Tests were conducted to find out whether the expression of artificial RNAs targeting the suppressors *CP* and *p6* could counteract the suppressor function and confer resistance to OMMV using hairpin constructs. Two hairpin constructs targeting the *p6* and the *CP* were agroinfiltrated in plants to transiently express long pathogen-related dsRNAs and pre-activate plant RNA silencing machinery through the procession of dsRNAs into siRNAs that are responsible for the degradation of invading viral RNA.

For the construction of the *p6* hairpin, the full *p6* was used; for the *CP* hairpin construct, the first 141 nt of the *CP* were removed (OMMV *CP*minus141) in order to reduce the potential biosafety risks associated with the production of *CP* molecules, as well as exclude *CP*-mediated resistance events; still, a long fragment was used so that a higher number of potentially active virus-specific siRNAs would be present and specifically target the coding region of *CP*.

This study shows that the expression of OMMV *CP*minus141 and OMMV *p6* interfered with the multiplication of OMMV, as the plants expressing them resulted in a highly substantial reduction in viral accumulation and symptoms attenuation, proving their effectiveness against OMMV infection. The percentage of resistant plants obtained in this study (60%) is similar to the highest percentages of viral resistance obtained in other studies [50,53,54].

Plants transiently expressing OMMV CPminus141 interfered with the multiplication of OMMV; however, it was not as effective against OMMV infection as plants expressing both that and OMMV p6, as just 20% of the plants were OMMV-resistant. No resistant plants were obtained when OMMV p6 was being expressed; however, a slight delay in the appearance of symptoms occurred when compared to the control. These results show that OMMV can counteract these mechanisms by inhibiting silencing. Only when plants expressed both OMMV suppressors, CP and p6, was a high efficient RNA silencing mechanism triggered. This has also been observed for CTV, where resistance is only achieved when the three viral silencing suppressors were targeted simultaneously [55].

The findings obtained here contribute to the knowledge on resistance induction frequencies, and are of great importance for the future development of OMMV-resistant plants that are either transgenic or, as an alternative, in transient systems by directly delivering RNA-silencing molecules into plants, as to overcome the lack of a regulatory framework and the strong opposition associated with transgenic plants. Additionally, resistance to other closely related viruses may be achieved, as viruses with less than 15–20% difference at the sequence level may confer protection to each other [56,57]. Such small differences exist between OMMV and other necroviruses such as TNV-D and OLV-1, whose co-infections are frequent in nature [58]. It is common for plants to be invaded by several viruses, and this study shows the most efficient OMMV transgenes that confer resistance to OMMV, which may be used in multiple combined sequences assembled with other viruses that are expected to infect the crop to achieve protection and a broader resistance against a wide range of viruses.

Besides helping understandings of the interaction between viruses and hosts, the knowledge on viral suppressors may also have other commercial impacts, as in the production of heterologous proteins using bioreactor plants. Host RNA silencing has shown to reduce the efficiency of gene expression in plants [59]. In this way, the co-expression of a silencing suppressor and the target gene may be an attractive option to reduce problems in transgene expression. This is essential to respond to the continuous increase in the demand to produce large amounts of recombinant proteins for the industry, for which plants are one of the most effective and safe systems for large-scale production.

Author Contributions: Conceptualization, C.M.V., G.N. and M.d.R.F.; Methodology, C.M.V., P.M. and M.d.R.F.; Statistical Analysis, P.M.; Investigation, C.M.V., P.M., G.N., M.d.R.F.; Resources, M.d.R.F.; Writing—Original Draft Preparation, C.M.V.; Writing—Review & Editing, C.M.V., P.M., M.D.C., M.I.E.C., G.N., M.d.R.F.; Funding Acquisition, C.M.V., P.M., M.d.R.F.

Funding: This work was funded by National Funds through FCT-Foundation for Science and Technology under the Project UID/AGR/00115/2013, by the European Union through the European Regional Development Fund, under the ALENTEJO 2020 (Regional Operational Program of the Alentejo) through the project Enhancing the Performance of Portuguese Olive Cultivars (OLEAVALOR) ALT20-03-0145-FEDER-000014, and by the project “Control of olive anthracnose through gene silencing and gene expression using a plant virus vector” with the reference ALT20-03-0145-FEDER-028263 and the project “Development of a new virus-based vector to control TSWV in tomato plants” with the reference ALT20-03-0145-FEDER-028266, co-financed by the European Union through the European Regional Development Fund, under the ALENTEJO 2020 (Regional Operational Program of the Alentejo), ALGARVE 2020 (Regional Operational Program of the Algarve) and through the Foundation for Science and Technology, in its national component. C. Varanda was supported by a post-doctoral fellowship (SFRH/BPD/76194/2011) from the Foundation for Science and Technology (FCT), funded by QREN—POPH—Typology 4.1—co-funded by MES National Funding and The European Social Fund.

Acknowledgments: The authors would like to thank CSIRO for providing pHELLSGATE vector.

Conflicts of Interest: The authors declare no conflict of interest. The funding sponsors had no role in the design of the study; in the collection, analyses, or interpretation of data; in the writing of the manuscript, and in the decision to publish the results.

References

1. Voinnet, O. RNA silencing as a plant immune system against viruses. *Trends Genet.* **2001**, *17*, 449–459. [[CrossRef](#)]
2. Baulcombe, D. RNA silencing in plants. *Nature* **2004**, *431*, 356–363. [[CrossRef](#)] [[PubMed](#)]

3. Kontra, L.; Csorba, T.; Tavazza, M.; Lucioli, A.; Tavazza, R.; Moxon, S.; Tisza, V.; Medzihradsky, A.; Turina, M.; Burgyán, J. Distinct effects of p19 RNA silencing suppressor on small RNA mediated pathways in plants. *PLoS Pathog.* **2016**, *12*, e1005935. [[CrossRef](#)] [[PubMed](#)]
4. Carbonell, A.; Carrington, J.C. Antiviral roles of plant argonautes. *Curr. Opin. Plant Biol.* **2015**, *27*, 111–117. [[CrossRef](#)] [[PubMed](#)]
5. Brodersen, P.; Voinnet, O. The diversity of RNA silencing pathways in plants. *Trends Genet.* **2006**, *22*, 268–280. [[CrossRef](#)] [[PubMed](#)]
6. Ding, S.W.; Voinnet, O. Antiviral immunity directed by small RNAs. *Cell* **2007**, *130*, 413–426. [[CrossRef](#)] [[PubMed](#)]
7. Wassenegger, M.; Krczal, G. Nomenclature and functions of RNA-directed RNA polymerases. *Trends Plant Sci.* **2006**, *11*, 142–151. [[CrossRef](#)] [[PubMed](#)]
8. Pumpilin, N.; Voinnet, O. RNA silencing suppression by plant pathogens: Defence, counter-defence and counter-counter-defence. *Nat. Rev. Microbiol.* **2013**, *11*, 745–760. [[CrossRef](#)] [[PubMed](#)]
9. Csorba, T.; Kontra, L.; Burgyan, J. Viral silencing suppressors: Tools forged to finetune host-pathogen coexistence. *Virology* **2015**, *479*, 85–103. [[CrossRef](#)] [[PubMed](#)]
10. Burgyán, J.; Havelda, Z. Viral suppressors of RNA silencing. *Trends Plant Sci.* **2011**, *16*, 265–272. [[CrossRef](#)] [[PubMed](#)]
11. Samuel, G.H.; Wiley, M.R.; Badawi, A.; Adelman, Z.N.; Myles, K.M. Proceedings of the national academy of sciences of the united states of america. *Proc. Natl. Acad. Sci. USA* **2016**, *113*, 13863–13868. [[CrossRef](#)] [[PubMed](#)]
12. Silhavy, D.; Molnar, A.; Lucioli, A.; Szittyá, G.; Hornyik, C.; Tavazza, M.; Burgyan, J. A viral protein suppresses RNA silencing and binds silencing-generated, 21- to 25-nucleotide double-stranded RNAs. *EMBO J.* **2002**, *21*, 3070–3080. [[CrossRef](#)] [[PubMed](#)]
13. Chapman, E.J.; Prokhnevsky, A.I.; Gopinath, K.; Dojia, V.V.; Carrington, J.C. Viral RNA silencing suppressors inhibit the microRNA pathway at an intermediate step. *Genes Dev.* **2004**, *18*, 1179–1186. [[CrossRef](#)] [[PubMed](#)]
14. Lakatos, L.; Csorba, T.; Pantaleo, V.; Chapman, E.J.; Carrington, J.C.; Liu, Y.P.; Dolja, V.V.; Calvino, L.F.; Lopez-Moya, J.J.; Burgyan, J. Small RNA binding is a common strategy to suppress RNA silencing by several viral suppressors. *EMBO J.* **2006**, *25*, 2768–2780. [[CrossRef](#)] [[PubMed](#)]
15. Merai, Z.; Kerenyi, Z.; Molnar, A.; Barta, E.; Valoczi, A.; Bisztray, G.; Havelda, Z.; Burgyan, J.; Silhavy, D. Aureusvirus p14 is an efficient RNA silencing suppressor that binds double-stranded RNAs without size specificity. *J. Virol.* **2005**, *79*, 7217–7226. [[CrossRef](#)] [[PubMed](#)]
16. Qu, F.; Ren, T.; Morris, T.J. The coat protein of turnip crinkle virus suppresses posttranscriptional gene silencing at an early initiation step. *J. Virol.* **2003**, *77*, 511–522. [[CrossRef](#)] [[PubMed](#)]
17. Zhang, F.; Simon, A.E. Enhanced viral pathogenesis associated with a virulent mutant virus or a virulent satellite RNA correlates with reduced virion accumulation and abundance of free coat protein. *Virology* **2003**, *312*, 8–13. [[CrossRef](#)]
18. Powers, J.G.; Sit, T.L.; Heinsohn, C.; George, C.G.; Kim, K.-H.; Lommel, S.A. The red clover necrotic mosaic virus RNA-2 encoded movement protein is a second suppressor of RNA silencing. *Virology* **2008**, *381*, 277–286. [[CrossRef](#)] [[PubMed](#)]
19. Takeda, A.; Tsukuda, M.; Mizumoto, H.; Okamoto, K.; Kaido, M.; Mise, K.; Okuno, T. A plant RNA virus suppresses RNA silencing through viral RNA replication. *EMBO J.* **2005**, *24*, 3147–3157. [[CrossRef](#)] [[PubMed](#)]
20. Saponari, M.; Alkowni, R.; Grieco, F.; Pantaleo, V.; Savino, V.; Martelli, G.P.; Driouech, N.; Hassan, M.; Di Terlizzi, B.; Digiario, M. Detection of olive-infecting viruses in the mediterranean basin. In Proceedings of the Fourth International Symposium on Olive Growing, Valenzano, Italy, 25–30 September 2000; pp. 787–790.
21. Varanda, C.; Félix, M.R.F.; Leitão, F.; Sismeiro, R.; Clara, M.I.E. Application of reverse transcription—Polymerase chain reaction to screen a collection of clones of *Olea europaea* L. For the presence of necroviruses (tombusviridae). In Proceedings of the 8th Conference of the European Foundation for Plant Pathology & British Society of Plant Pathology Presidential Meeting 2006, Frederiksberg, Denmark, 13–17 August 2006.
22. El Air, M.; Mahfoudi, N.; Digiario, M.; Najjar, A.; Elbeaino, T. Detection of olive infecting viruses in tunisia. *J. Phytopathol.* **2011**, *159*, 283–286. [[CrossRef](#)]
23. Cardoso, J.; Félix, M.; Clara, M.; Oliveira, S. The complete genome sequence of a new necrovirus isolated from *Olea europaea* L. *Arch. Virol.* **2005**, *150*, 815–823. [[CrossRef](#)] [[PubMed](#)]

24. Varanda, C.; Félix, M.; Soares, C.; Oliveira, S.; Clara, M. Specific amino acids of olive mild mosaic virus coat protein are involved on transmission by *Olpidium brassicae*. *J. Gen. Virol.* **2011**, *92*, 2209–2213. [[CrossRef](#)] [[PubMed](#)]
25. Cardoso, J.M.S.; Felix, M.R.; Clara, M.I.E.; Oliveira, S. First characterization of infectious cDNA clones of olive mild mosaic virus. *Phytopathol. Mediterr.* **2012**, *51*, 259–265.
26. Karimi, M.; Inze, D.; Depicker, A. Gateway vectors for *Agrobacterium*-mediated plant transformation. *Trends Plant Sci.* **2002**, *7*, e193–e195. [[CrossRef](#)]
27. Haseloff, J.; Siemering, K.R.; Prasher, D.C.; Hodge, S. Removal of a cryptic intron and subcellular localization of green fluorescent protein are required to mark transgenic arabidopsis plants brightly. *Proc. Natl. Acad. Sci. USA* **1997**, *94*, 2122–2127. [[CrossRef](#)] [[PubMed](#)]
28. Costa, Â.; Marques, N.; Nolasco, G. Citrus tristeza virus p23 may suppress systemic silencing but is not related to the kind of viral syndrome. *Physiol. Mol. Plant Pathol.* **2014**, *87*, 69–75. [[CrossRef](#)]
29. Brigneti, G.; Voinnet, O.; Li, W.X.; Ji, L.H.; Ding, S.W.; Baulcombe, D.C. Viral pathogenicity determinants are suppressors of transgene silencing in *Nicotiana benthamiana*. *EMBO J.* **1998**, *17*, 6739–6746. [[CrossRef](#)] [[PubMed](#)]
30. Liu, D.; Shi, L.; Han, C.; Yu, J.; Li, D.; Zhang, Y. Validation of reference genes for gene expression studies in virus-infected *Nicotiana benthamiana* using quantitative real-time PCR. *PLoS ONE* **2012**, *7*, e46451. [[CrossRef](#)] [[PubMed](#)]
31. Clarke, K.R.; Warwick, R.M. *Changes in Marine Communities: An Approach to Statistical Analysis and Interpretation*, 2nd ed.; PRIMER-E Ltd.: Plymouth, UK, 2001.
32. Anderson, M.J.; Gorley, R.N.; Clarke, K.R. *Permanova a+ for Primer: Guide to Software and Statistical Methods*; PRIMER-E: Plymouth, UK, 2008.
33. Clarke, K.; Green, R. Statistical design and analysis for a biological effects study. *Mar. Ecol. Prog. Ser.* **1988**, *46*, 213–226. [[CrossRef](#)]
34. Zhang, L.; French, R.; Langenberg, W.G. Molecular cloning and sequencing of the coat protein gene of a nebraskan isolate of tobacco necrosis virus. The deduced coat protein sequence has only moderate homology with those of strain A and strain D. *Arch. Virol.* **1993**, *132*, 291–305. [[CrossRef](#)] [[PubMed](#)]
35. Eamens, A.L.; Waterhouse, P.M. Vectors and methods for hairpin RNA and artificial microRNA-mediated gene silencing in plants. *Methods Mol. Biol.* **2011**, *701*, 179–197. [[PubMed](#)]
36. Family-tombusviridae. In *Virus Taxonomy*; Elsevier: San Diego, CA, USA, 2012; pp. 1111–1138.
37. Lu, R.; Folimonov, A.; Shintaku, M.; Li, W.-X.; Falk, B.W.; Dawson, W.O.; Ding, S.-W. Three distinct suppressors of RNA silencing encoded by a 20-kb viral RNA genome. *Proc. Natl. Acad. Sci. USA* **2004**, *101*, 15742–15747. [[CrossRef](#)] [[PubMed](#)]
38. Gupta, A.K.; Hein, G.L.; Graybosch, R.A.; Tatineni, S. Octapartite negative-sense RNA genome of high plains wheat mosaic virus encodes two suppressors of RNA silencing. *Virology* **2018**, *518*, 152–162. [[CrossRef](#)] [[PubMed](#)]
39. Mlotshwa, S.; Voinnet, O.; Mette, M.F.; Matzke, M.; Vaucheret, H.; Ding, S.W.; Pruss, G.; Vance, V.B. RNA silencing and the mobile silencing signal. *Plant Cell* **2002**, *14*, S289–S301. [[CrossRef](#)] [[PubMed](#)]
40. Bag, S.; Mitter, N.; Eid, S.; Pappu, H.R. Complementation between two tospoviruses facilitates the systemic movement of a plant virus silencing suppressor in an otherwise restrictive host. *PLoS ONE* **2012**, *7*, e44803. [[CrossRef](#)] [[PubMed](#)]
41. Flores, R.; Ruiz-Ruiz, S.; Soler, N.; Sanchez-Navarro, J.; Fagoaga, C.; Lopez, C.; Navarro, L.; Moreno, P.; Peña, L. Citrus tristeza virus p23: A unique protein mediating key virus-host interactions. *Front. Microbiol.* **2013**, *4*, 1–9. [[CrossRef](#)] [[PubMed](#)]
42. Pruss, G.; Ge, X.; Shi, X.M.; Carrington, J.C.; Vance, V.B. Plant viral synergism: The potyviral genome encodes a broad-range pathogenicity enhancer that transactivates replication of heterologous viruses. *Plant Cell* **1997**, *9*, 859–868. [[CrossRef](#)] [[PubMed](#)]
43. Felix, M.; Varanda, C.; Clara, M. Biology and molecular characterization of necroviruses affecting *Olea europaea* L.: A review. *Eur. J. Plant Pathol.* **2012**, *133*, 247–259. [[CrossRef](#)]
44. Molnar, A.; Havelda, Z.; Dalmay, T.; Szutorisz, H.; Burgyan, J. Complete nucleotide sequence of tobacco necrosis virus strain DH and genes required for RNA replication and virus movement. *J. Gen. Virol.* **1997**, *78*, 1235–1239. [[CrossRef](#)] [[PubMed](#)]

45. Lomonosoff, G.P. Pathogen-derived resistance to plant viruses. *Ann. Rev. Phytopathol.* **1995**, *33*, 323–343. [[CrossRef](#)] [[PubMed](#)]
46. Smith, H.A.; Swaney, S.L.; Parks, T.D.; Wernsman, E.A.; Dougherty, W.G. Transgenic plant virus resistance mediated by untranslatable sense RNAs: Expression, regulation, and fate of nonessential RNAs. *Plant Cell* **1994**, *6*, 1441–1453. [[CrossRef](#)] [[PubMed](#)]
47. Liu, H.M.; Zhu, C.X.; Zhu, X.P.; Guo, X.Q.; Song, Y.Z.; Wen, F.J. A link between PVY^N CP gene-mediated virus resistance and transgene arrangement. *J. Phytopathol.* **2007**, *155*, 676–682. [[CrossRef](#)]
48. Tenllado, F.; Diaz-Ruiz, J.R. Double-stranded RNA-mediated interference with plant virus infection. *J. Virol.* **2001**, *75*, 12288–12297. [[CrossRef](#)] [[PubMed](#)]
49. Simon-Mateo, C.; Garcia, J.A. MicroRNA-guided processing impairs Plum pox virus replication, but the virus readily evolves to escape this silencing mechanism. *J. Virol.* **2006**, *80*, 2429–2436. [[CrossRef](#)] [[PubMed](#)]
50. Konakalla, N.C.; Kaldis, A.; Berbati, M.; Masarapu, H.; Voloudakis, A.E. Exogenous application of double-stranded RNA molecules from TMV p126 and CP genes confers resistance against TMV in tobacco. *Planta* **2016**, *244*, 961–969. [[CrossRef](#)] [[PubMed](#)]
51. Smith, N.A.; Singh, S.P.; Wang, M.B.; Stoutjesdijk, P.A.; Green, A.G.; Waterhouse, P.M. Total silencing by intron-spliced hairpin RNAs. *Nature* **2000**, *407*, 319–320. [[CrossRef](#)] [[PubMed](#)]
52. Wesley, S.V.; Helliwell, C.A.; Smith, N.; Wang, M.; Rouse, D.T.; Liu, Q.; Gooding, P.S.; Singh, S.P.; Abbott, D.; Stoutjesdijk, P.A.; et al. Construct design for efficient, effective and high throughput gene silencing in plants. *Plant J.* **2001**, *27*, 581–590. [[CrossRef](#)] [[PubMed](#)]
53. Hily, J.M.; Ravelonandro, M.; Damsteegt, V.; Bassett, C.; Petri, C.; Liu, Z.; Scorza, R. Plum pox virus coat protein gene intron hairpin-RNA (ihpRNA) constructs provide resistance to Plum pox virus in *Nicotiana benthamiana* and *Prunus domestica*. *J. Am. Soc. Hortic. Sci.* **2017**, *132*, 850–858.
54. Di Nicola-Negri, E.; Brunetti, A.; Tavazza, M.; Ilardi, V. Hairpin RNA-mediated silencing of Plum pox virus P1 and HC-Pro genes for efficient and predictable resistance to the virus. *Transgen. Res.* **2005**, *14*, 989–994. [[CrossRef](#)] [[PubMed](#)]
55. Roy, G.; Sudarshana, M.R.; Ullman, D.E.; Ding, S.W.; Dandekar, A.M.; Falk, B.W. Chimeric cDNA sequences from citrus tristeza virus confer RNA silencing-mediated resistance in transgenic *Nicotiana benthamiana* plants. *Phytopathology* **2006**, *96*, 819–827. [[CrossRef](#)] [[PubMed](#)]
56. Jones, A.L.; Thomas, C.L.; Maule, A.J. De novo methylation and co-suppression induced by a cytoplasmically replicating plant RNA virus. *EMBO J.* **1998**, *17*, 6385–6393. [[CrossRef](#)] [[PubMed](#)]
57. Duan, C.G.; Fang, Y.Y.; Zhou, B.J.; Zhao, J.H.; Hou, W.N.; Zhu, H.; Ding, S.W.; Guo, H.S. Suppression of arabidopsis ARGONAUTE1-mediated slicing, transgene-induced RNA silencing, and DNA methylation by distinct domains of the cucumber mosaic virus 2b protein. *Plant Cell* **2012**, *24*, 259–274. [[CrossRef](#)] [[PubMed](#)]
58. Varanda, C.; Cardoso, J.; Félix, M.; Oliveira, S.; Clara, M. Multiplex RT-PCR for detection and identification of three necroviruses that infect olive trees. *J. Plant Pathol.* **2010**, *127*, 161–164. [[CrossRef](#)]
59. Ma, P.; Liu, J.; He, H.; Yang, M.; Li, M.; Zhu, X.; Wang, X. A viral suppressor P1/HC-pro increases the GFP gene expression in *Agrobacterium*-mediated transient assay. *Appl. Biochem. Biotechnol.* **2009**, *158*, 243–252. [[CrossRef](#)] [[PubMed](#)]

